Stationary spatial patterns in passive optical systems: Two-level atoms

L. A. Lugiato and C. Oldano
Dipartimento di Fisica del Politecnico, Corso Duca degli Abruzzi 24, 10129 Torino, Italy
(Received 25 June 1987)

We discuss a novel type of optical instability, which leads to the spontaneous formation of a stationary spatial structure, instead of to the onset of oscillations or pulsations. A passive system is contained in an optical cavity, to which we add two lateral mirrors. Under appropriate conditions, diffraction of radiation can induce the onset of a transverse-stripe structure in an initially uniform plane-wave field configuration. In this paper, we consider the case of a homogeneously broadened two-level system. The model on which our analysis is based is derived from the Maxwell-Bloch equations in the paraxial approximation, using the mean-field limit and assuming a large Fresnel number. We show that, with respect to the bistability parameter C, the threshold of the spatial instability coincides with the bistability threshold for absorptive, resonant optical bistability. The spatial instability requires, however, a detuned configuration and can arise both in the absence and presence of bistability. In the latter case, it can occur both in the lower and in the upper branch of the steady-state curve. The instability is caused by competition between different transverse modes, which realize a situation of spatial coexistence, different from the state of temporal coexistence which characterizes the spontaneous oscillations that arise from the previously known multimode instabilities. Finally, we discuss some points relevant for an experimental observation of this phenomenon.

I. INTRODUCTION

Recent years have witnessed a remarkable development in the field of optical instabilities.[1-8] The common features of these phenomena can be described as follows. One considers a system with constant parameters, maintained far from thermal equilibrium. Under normal conditions, its output approaches a time-stationary regime. However, for appropriate intervals of values for the control parameters, this stationary-state regime becomes unstable against random perturbations, and the system's output spontaneously starts to oscillate or pulsate. The long-time behavior which then establishes itself is regular (periodic), quasiperiodic, or chaotic according to the parameter values. From the viewpoint of linear-stability analysis, all these phenomena present an instability boundary (i.e., the boundary of the unstable domain in parameter space) characterized by the fact that a pair of complex-conjugate eigenvalues yield a vanishing real part (hard-mode instability). This solution gives rise to a Hopf bifurcation which produces the oscillatory state.

On the other hand, from the general theory (see, e.g., Refs. 9 and 10) we know that there are instabilities which follow different scenarios. These arise when the instability boundary or a part of it is characterized by the fact that a real eigenvalue vanishes (soft-mode instability). In this case, the system does not approach an oscillatory regime, but evolves towards a new stationary state qualitatively different from the original one.

Typically, the original or "normal" stationary state is homogeneous in space; however, the system is able to support also spatially inhomogeneous modes. If the instability arises from a homogeneous perturbation, the new stationary state is also homogeneous. Examples of phenomena of this kind in optics are the bifurcation of the lasing state at laser threshold[9] and the instability which gives rise to the phenomenon of optical bistability.[3]

The most interesting situations are those in which the instability arises from an inhomogeneous perturbation; in other words, the homogeneous stationary state becomes unstable against the growth of an inhomogeneous mode. In this case the new stationary state is nonuniform in space. Following Nicolis and Prigogine,[10] one has the spontaneous onset of a spatial dissipative structure, whereas in the case of Hopf birfurcation one has the rise of a temporal or a spatio-temporal dissipative structure.

Examples of spatial dissipative structures have been described, for instance, in nonlinear chemical reactions and in developmental biology.[9-11] However, to our knowledge, in the framework of optics it is only very recently[12] that the first model which explicitly displays a phenomenology of this type has been pointed out. In fact, in optical bistability, nice spatial patterns, both of transverse[13] and longitudinal[14] type, have been found previously in the switching process from the lower to the upper branch of the hysteresis curve. These phenomena which only occur in the bistability region, are however caused by a different mechanism from that which gives rise to a spatial dissipative structure. The model formulated in Ref. 12 has the same degree of simplicity as the model "Brussellator;"[10] here, however, the spatial patterns do not arise from diffusion but from diffraction.

The aim of this article is twofold. First, we want to give the derivation of the model from first principles and illustrate in detail the analysis which produces the results sketchily described in Ref. 12. Second, the model proposed in Ref. 12 holds for a Kerr medium or for a two-level system in the purely dispersive limit. We want to extend it to the general case of a two-level system with both absorption and dispersion.

This work is divided into two parts. In this paper we

show the derivation of the general model for a two-level system in the mean-field limit, including diffraction, both for a ring and for a Fabry-Perot cavity. Furthermore, we perform in detail the linear-stability analysis for a ring cavity and prove that, with respect to the bistability parameter C, the instability threshold for the spatial pattern formation coincides with the bistability threshold $C=4$. In a future paper we will focus on the purely dispersive limit considered in Ref. 12 and perform a constructive analytical treatment of the bifurcation of nonuniform patterns from the spatially homogeneous stationary solution. In Sec. II we recall the two-level model of optical bistability for a ring cavity, from which, in Sec. III, we derive the set of modal equations for the amplitudes of the longitudinal modes. The resulting equations are generalized to the case of a Fabry-Perot cavity in Sec. IV. After introducing the single-longitudinal-mode approximation, in Sec. V we recover the well-known transversally homogeneous stationary solutions of the problem. In Sec. VI we add two side mirrors to the cavity and define precise transverse boundary conditions. Section VII describes the linear-stability analysis and proves the existence of an instability which leads to the onset of stationary spatial patterns in the transverse direction. The instability domain in parameter space is analyzed in detail in Sec. VIII. Section IX discusses briefly the instabilities, displayed by our model, which lead to the onset of temporal or spatio-temporal structures. In Sec. X we discuss our model in the limit of adiabatic elimination of the atomic variables, and in Sec. XI we illustrate the physical origin of the soft-mode spatial instability. Finally, in Sec. XII we discuss how the reflecting boundary conditions on the side mirrors, assumed in Sec. VI, can be realized in a real experiment.

II. THE TWO-LEVEL MODEL OF OPTICAL BISTABILITY, RING CAVITY

A two-level sample with N atoms, length L, and volume V is contained in the ring cavity of length $\mathcal{L}$ described in Fig. 1. Mirrors 1 and 4 have transmissivity coefficient T and reflectivity coefficient $R=1-T$; the other mirrors have 100% reflectivity. The longitudinal coordinate z is measured along the ring; hence mirror 1 has coordinate $z=0$ at the beginning of the loop and $z=\mathcal{L}$ at the end; mirror 4 corresponds to $z=L$. The part of the cavity from $z=0$ to $z=L$ contains the atomic medium, homogeneously distributed; the portion from $z=L$ to $z=\mathcal{L}$ is empty. The atomic system is homogeneously broadened and we call $\gamma_\parallel$ the relaxation rate of the population difference and $\gamma_\perp$ the relaxation rate of the atomic polarization, which coincides with the atomic linewidth. A coherent, plane-wave stationary field E_I of frequency ω_0 is injected into the cavity and is partially transmitted and partially reflected by the system. We consider the Rabi frequencies of the internal cavity field and of the input field,

$$\Omega(x,y,z,t)=\frac{\boldsymbol{\mu}\cdot\mathbf{E}(x,y,z,t)}{\hbar}\ ,$$
$$\Omega_I(t)=\frac{\boldsymbol{\mu}\cdot\mathbf{E}_I(t)}{\hbar}\ , \tag{1}$$

where $\boldsymbol{\mu}$ is the dipole moment of the atomic transition and x,y are the transverse space coordinates. We introduce the slowly varying approximation by setting

$$\Omega(x,y,z,t)=(\gamma_\perp\gamma_\parallel)^{1/2}F(x,y,z,t)\exp[i(k_0z-\omega_0t)]+\text{c.c.},$$
$$\Omega_I(t)=(\gamma_\perp\gamma_\parallel T)^{1/2}Y\exp(-i\omega_0t)+\text{c.c.}\ , \tag{2}$$

where F varies with respect to z and t much more slowly than the exponential factor and where $k_0=\omega_0/c$. For the sake of definiteness we assume that the normalized incident field Y is real and positive. Similarly, we introduce the slowly varying approximation for the atomic polarization $\mathcal{P}(x,y,z,t)$,

$$\mathcal{P}(x,y,z,t)=i\frac{\mu}{V}\left[\frac{\gamma_\parallel}{\gamma_\perp}\right]^{1/2}NP(x,y,z,t)\exp[i(k_0z-\omega_0t)]$$
$$+\text{c.c.}\ , \tag{3}$$

and normalize the quantity $\mathcal{D}(x,y,z,t)$, which represents the difference between the population of the lower and of the upper level,

$$\mathcal{D}(x,y,z,t)=ND(x,y,z,t)\ . \tag{4}$$

In the dipole and rotating wave approximation, the equations which govern the time evolution are

$$\frac{1}{2ik_0}\nabla_\perp^2F+\frac{\partial F}{\partial z}+\frac{1}{c}\frac{\partial F}{\partial t}=-\alpha P\ , \tag{5a}$$

$$\frac{\partial P}{\partial t}=\gamma_\perp[DF-P(1+i\Delta)]\ , \tag{5b}$$

$$\frac{\partial D}{\partial t}=-\frac{\gamma_\parallel}{2}(PF^*+FP^*+2D-2)\ , \tag{5c}$$

where $\nabla_\perp^2$ is the transverse Laplacian

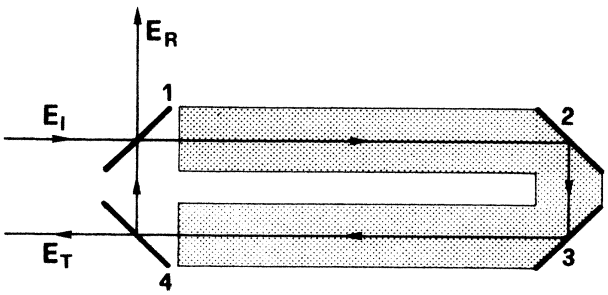

FIG. 1. Ring cavity filled with a passive medium. Mirrors 1 and 4 have transmissivity coefficient $T\ll 1$, mirrors 2 and 3 have 100% reflectivity. E_I, E_T, and E_R are the incident, transmitted, and reflected fields, respectively.

$$\nabla_\perp^2=\frac{\partial^2}{\partial x^2}+\frac{\partial^2}{\partial y^2} \tag{6}$$

and α is the unsaturated absorption coefficient of the field on resonance

$$\alpha=\frac{2\pi\mu^2 k_0 N}{\hbar\gamma_\perp V} \ . \tag{7}$$

The atomic detuning parameter Δ is given by

$$\Delta=(\omega_a-\omega_0)/\gamma_\perp \ , \tag{8}$$

where ω_a is the atomic transition frequency. The ring cavity is characterized by the following boundary condition:

$$F(x,y,0,t)=TY+R^{1/2}e^{-i\delta_0}F(x,y,\mathcal{L},t) \ , \tag{9}$$

The cavity detuning parameter δ_0 is given by

$$\delta_0=(\omega_c-\omega_0)T/k \ , \tag{10}$$

where ω_c is the frequency of the longitudinal cavity mode nearest to ω_0 (resonant mode) and k is the cavity linewidth defined as

$$k=cT/\mathcal{L} \ . \tag{11}$$

For the sake of simplicity we neglect the variation of the field in the short empty part of the cavity, and replace $F(x,y,\mathcal{L},t)$ by $R^{1/2}F(x,y,L,t)$. Thus Eq. (9) becomes

$$F(x,y,0,t)=TY+Re^{-i\delta_0}F(x,y,L,t) \ . \tag{12}$$

Accordingly, in the following we will systematically replace $\mathcal{L}$ by L in the expressions of the cavity linewidth (Eq. 11) and of the mode frequencies. Next we introduce the following changes of independent variables:[15]

$$\begin{aligned}\tilde{F}&=\exp\left[\frac{z}{L}(\ln R-i\delta_0)\right]F+T\frac{z}{L}Y \ ,\\ \tilde{P}&=\exp\left[\frac{z}{L}(\ln R-i\delta_0)\right]P \ ,\\ \tilde{D}&=D \ ,\end{aligned} \tag{13}$$

so that the dynamical equations become

$$\frac{1}{2ik_0}\nabla_\perp^2\tilde{F}-\frac{1}{L}(\ln R-i\delta_0)\left[\tilde{F}-T\frac{z}{L}Y\right]+\frac{\partial\tilde{F}}{\partial z}-\frac{T}{L}Y+\frac{1}{c}\frac{\partial\tilde{F}}{\partial t}=-\alpha\tilde{P} \ , \tag{14a}$$

$$\frac{\partial\tilde{P}}{\partial t}=-\gamma_\perp\left[\tilde{D}\left[\tilde{F}-T\frac{z}{L}Y\right]-\tilde{P}(1+i\Delta)\right] \ , \tag{14b}$$

$$\frac{\partial\tilde{D}}{\partial t}=-\frac{\gamma_\parallel}{2}\left[\tilde{P}\left[\tilde{F}^*-T\frac{zY}{L}\right]+\tilde{P}^*\left[\tilde{F}-T\frac{zY}{L}\right]\times\exp\left[-\frac{2z}{L}(\ln R-i\delta_0)\right]+2\tilde{D}-2\right] \ , \tag{14c}$$

while the boundary condition (12) takes the simple form of a periodicity condition in space,

$$\tilde{F}(x,y,0,t)=\tilde{F}(x,y,L,t) \ . \tag{15}$$

Next we introduce the mean-field limit[3]

$$\alpha L\ll 1, \quad T\ll 1, \quad \delta_0\ll 1 \tag{16}$$

with

$$C=\frac{\alpha L}{2T} \quad \text{(arbitrary)} \tag{17a}$$

and

$$\theta=\delta_0/T \quad \text{(arbitrary)} \ , \tag{17b}$$

in which the set of equations (14) takes the simpler form

$$\frac{\partial\tilde{F}}{\partial t}+c\frac{\partial\tilde{F}}{\partial z}=k[-i\theta\tilde{F}-(\tilde{F}-Y)-2C\tilde{P}]+\frac{ic}{2k_0}\nabla_\perp^2\tilde{F} \ , \tag{18a}$$

$$\frac{\partial\tilde{P}}{\partial t}=\gamma_\perp[\tilde{F}\tilde{D}-(1+i\Delta)\tilde{P}] \ , \tag{18b}$$

$$\frac{\partial\tilde{D}}{\partial t}=-\gamma_\parallel[\tfrac{1}{2}(\tilde{F}\tilde{P}^*+\tilde{F}^*P)+\tilde{D}-1] \ . \tag{18c}$$

III. THE MODAL EQUATIONS AND THE SINGLE LONGITUDINAL MODE APPROXIMATION

Following a quite common procedure in quantum optics, we reformulate Eqs. (18) in terms of mode variables. The longitudinal cavity frequencies are $\omega_c+\alpha_m$, where ω_c is the frequency nearest to ω_0 and

$$\alpha_m=\frac{2\pi c}{L}m, \quad m=0,\pm1,\pm2,\ldots \ . \tag{19}$$

We introduce the following expansions in longitudinal modes:

$$\begin{pmatrix}\tilde{F}(x,y,z,t')\\ \tilde{P}(x,y,z,t')\\ \tilde{D}(x,y,z,t')\end{pmatrix}=\sum_m\exp(ik_m z)\begin{pmatrix}f_m(x,y,t')\\ p_m(x,y,t')\\ d_m(x,y,t')\end{pmatrix} \ , \tag{20}$$

with

$$k_m=\frac{\alpha_m}{c}=\frac{2\pi}{L}m \ . \tag{21}$$

The functions $\exp(ik_m z)$ obey the periodicity condition (15). On substituting Eq. (20) into Eqs. (18) and taking into account the orthogonality of the function $\exp(ik_m z)$ in the interval $0\le z\le L$, one finds the following equations for the modal amplitudes f_m,p_m,d_m:

$$\frac{\partial f_m}{\partial t}=-i\alpha_m f_m+k[-i\theta f_m-(f_m-Y\delta_{m,0})-2Cp_m]+i\frac{c}{2k_0}\nabla_\perp^2 f_m \ , \tag{22a}$$

$$\frac{\partial p_m}{\partial t}=\gamma_\perp\left[\sum_{m'}f_{m'}d_{m-m'}-(1+i\Delta)p_m\right] \ , \tag{22b}$$

$$\frac{\partial d_m}{\partial t}=-\gamma_{\parallel}\left[\frac{1}{2}\sum_{m'}(f_{m'}p^*_{m'-m}+f^*_{m'}p_{m+m'})+d_m-\delta_{m,0}\right] . \tag{22c}$$

When the fields $\tilde{F}$, $\tilde{P}$, and $\tilde{D}$ are uniform with respect to the longitudinal variable z, only the amplitudes f_0, p_0, and d_0 corresponding to the resonant longitudinal mode $m=0$ are different from zero. Note from Eqs. (22) that if the fields are initially independent of z, they keep this property during the whole evolution. In this paper we will assume that the longitudinal-mode spacing $2\pi c/L$ is much larger than the atomic linewidth $\gamma_{\perp}$, and the resonant longitudinal mode $m=0$ is the nearest to the center of the atomic line. In these conditions, the modes with $m\neq 0$ cannot be appreciably excited, hence Eqs. (22) reduce to

$$\frac{\partial f_0}{\partial t}=k[-i\theta f_0-(f_0-Y)-2Cp_0]+i\frac{c}{2k_0}\nabla_{\perp}^2 f_0 , \tag{23a}$$

$$\frac{\partial p_0}{\partial t}=\gamma_{\perp}[f_0 d_0-(1+i\Delta)p_0] , \tag{23b}$$

$$\frac{\partial d_0}{\partial t}=-\gamma_{\parallel}[\tfrac{1}{2}(f_0 p_0^*+f_0^* p_0)+d_0-1] . \tag{23c}$$

Clearly, Eqs. (23) give a single-longitudinal-mode theory.

IV. THE TWO-LEVEL MODEL OF OPTICAL BISTABILITY, FABRY-PEROT CAVITY

In this section we will consider, instead of a ring cavity, a Fabry-Perot cavity of length L (Fig. 2). The derivation of the single-longitudinal-mode equations, analogous to Eqs. (23), is shown in detail in Ref. 16. In this approximation the Rabi frequency of the internal cavity field is proportional to

$$f_0(x,y,t)\cos(k_c z)\exp(-i\omega_0 t)+\text{c.c.} , \tag{24}$$

where $k_c=\omega_c/c$ is the wave number of the longitudinal cavity mode whose frequency is nearest to the input field frequency ω_0 (resonant mode). The dynamical equations read[16]

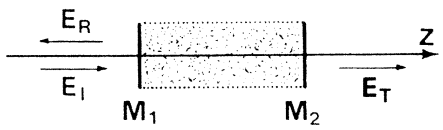

FIG. 2. Filled Fabry-Perot cavity. The mirrors M_1 and M_2 have transmissivity coefficient $T\ll 1$. E_I, E_T, and E_R are the incident, transmitted, and reflected fields, respectively.

$$\frac{\partial f_0}{\partial t}=k\left[-i\theta f_0-(f_0-Y)-2C\int_{-\pi}^{\pi}d\eta\cos(\eta)p_0(x,y,\eta,t)\right]+i\frac{c}{2k_c}\nabla_{\perp}^2 f_0 , \tag{25a}$$

$$\frac{\partial p_0}{\partial t}=\gamma_{\perp}[2f_0 d_0\cos\eta-(1+i\Delta)p_0] , \tag{25b}$$

$$\frac{\partial d_0}{\partial t}=-\gamma_{\parallel}[(f_0 p_0^*+f_0^* p_0)\cos\eta+d_0-1] , \tag{25c}$$

where the variable η takes into account the standing-wave structure of the longitudinal mode. The parameters k and C are defined as follows:

$$k=\frac{cT}{2L},\quad C=\frac{\alpha L}{T} . \tag{11'}$$

Here the field variable t_0 depends on x, y and t, whereas the atomic variables p_0 and d_0 depend on x, y, η, and t.

V. TRANSVERSALLY HOMOGENEOUS STATIONARY SOLUTIONS

Because the input field is a plane wave, Eqs. (23) admit stationary solutions which are transversally homogeneous, i.e., independent of x and y. One obtains

$$d_{0,s}=\frac{1+\Delta^2}{1+\Delta^2+|f_{0,s}|^2} , \tag{26a}$$

$$p_{0,s}=\frac{(1-i\Delta)f_{0,s}}{1+\Delta^2+|f_{0,s}|^2} , \tag{26b}$$

and on substituting Eq. (26b) into Eq. (23a) we find

$$Y=f_{0,s}\left[\left[1+\frac{2C}{1+\Delta^2+|f_{0,s}|^2}\right]+i\left[\theta-\frac{2C\Delta}{1+\Delta^2+|f_{0,s}|^2}\right]\right] , \tag{27}$$

from which we obtain the steady-state equation which links the input intensity Y^2 and the transmitted intensity

$$Y^2=I\left[\left[1+\frac{2C}{1+\Delta^2+I}\right]^2+\left[\theta-\frac{2C\Delta}{1+\Delta^2+I}\right]^2\right] , \tag{28}$$

where we defined

$$I=|f_{0,s}|^2 . \tag{28'}$$

If we plot I as a function of Y^2, according to the values of the parameters C, Δ, and θ we obtain a single-valued function or an S-shaped curve. The latter case corresponds to a bistable situation because the portion of the steady state with negative slope is unstable.[3] For given values of Δ and θ there is a threshold value $C_{\min}(\Delta,\theta)$ above which we obtain bistability. The explicit expression of $C_{\min}$ is given in Ref. 3. The function $C_{\min}(\Delta,\theta)$ attains its absolute minimum in the resonant case

$\Delta=\theta=0$, for which $C_{\min}=4$. In this sense, in the following we will refer to the value $C=4$ as the "bistability threshold." In the case of the Fabry-Perot cavity, Eqs. (25) lead to the following steady-state equation,[17,18] instead of Eq. (28):

$$Y^2=I\left[\left\{1+\frac{C}{I}\left[1-\left[\frac{1+\Delta^2}{1+\Delta^2+4I}\right]^{1/2}\right]\right\}^2+\left\{\theta-\frac{C\Delta}{I}\left[1-\left[\frac{1+\Delta^2}{1+\Delta^2+4I}\right]^{1/2}\right]\right\}^2\right] . \quad (29)$$

Also in this case one defines a function $C_{\min}(\Delta,\theta)$, which is discussed in Ref. 18.

VI. BOUNDARY CONDITIONS FOR THE TRANSVERSE VARIABLES

When the input field Y is a plane wave, it is also commonly assumed that the internal field is independent of x and y, and therefore the diffraction term in Eq. (23a) or Eq. (25a) drops. This assumption is, however, not always correct, as one immediately realizes by considering the stability of the homogeneous stationary solutions. In fact, the general perturbation, which probes the stability of the steady states, arises from a random fluctuation, and therefore is not necessarily uniform in the transverse direction. Hence the linear-stability analysis must be performed including the diffraction term. This necessity was clearly pointed out in Ref. 19.

Because Eqs. (23a) and (25a) present second derivatives with respect to the transverse coordinate, we must give the boundary conditions of the problem. Precisely, we include in our ring (Fig. 1) or the Fabry-Perot (Fig. 2) cavity configuration two additional mirrors orthogonal to the axis x, with a distance b and 100% reflectivity. The resulting configuration in the case of the Fabry-Perot cavity is shown in Fig. 3. Furthermore, we assume that both the input field and the internal cavity field are linearly polarized in the y direction; hence, due to the transversality condition, which prescribes that the divergence of the electric field vanishes, the internal field f_0 is independent of y, and Eq. (23a) reduces to

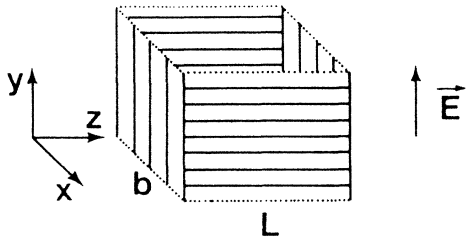

FIG. 3. Depicts the cavity configuration considered in Secs. V–XI. The two mirrors orthogonal to the axis z have transmissivity coefficient $T\ll 1$; the two mirrors orthogonal to the axis x have 100% reflectivity. The cavity is open in the y direction, which is also the direction of polarization of the electric field.

$$\frac{\partial f_0}{\partial t}=k[-i\theta f_0-(f_0-Y)-2Cp_0]+i\frac{c}{2k_0}\frac{\partial^2 f_0}{\partial x^2} , \quad (30)$$

while Eq. (25a) becomes

$$\frac{\partial f_0}{\partial t}=k\left[-i\theta f_0-(f_0-Y)-\frac{2C}{2\pi}\int_{-\pi}^{\pi}d\eta\cos(\eta)p_0(x,\eta,t)\right]+i\frac{c}{2k_c}\frac{\partial^2 f_0}{\partial x^2} , \quad (31)$$

and the quantities p_0, d_0, in both cases, do not depend on y. On the two mirrors orthogonal to the x axis, the field f_0 obeys reflecting boundary conditions which prescribe the vanishing of $\partial f_0/\partial x$. Therefore, the cavity modes that enter into play are (a) the ring cavity,

$$\cos(k_x x)\exp(ik_c z), \quad k_x=\frac{\pi}{b}n, \quad k_c=\frac{2\pi}{L}n_z , \quad (32a)$$

and (b) the Fabry-Perot cavity,

$$\cos(k_x x)\cos(k_c z), \quad k_x=\frac{\pi}{b}n, \quad k_c=\frac{\pi}{L}n_z , \quad (32b)$$

where $k_c=\omega_c/c$ is the longitudinal wave number of the resonant mode and n, n_z are non-negative integer numbers. Note that using Eqs. (30) and (31) we fix the value of n_z, whereas the integer n is free to vary in the range $0,1,2,\ldots$. Therefore we are dealing with a model which is single mode from a longitudinal viewpoint, but takes into account an infinite number of transverse modes. The stationary solutions governed by Eqs. (27) and (28) correspond to $n=0$; however, as we will show in Sec. VII, under appropriate conditions these solutions can become unstable against the growth of transverse modes with n larger than zero. In order to reduce the number of parameters in play to a minimum, it is convenient to normalize the independent variables. Precisely, we define

$$\bar{x}=x/b, \quad \bar{t}=kt . \quad (33)$$

Thus taking into account Eqs. (11) and the relation $k_c=2\pi/\lambda$, where λ is the wavelength, Eqs. (30), (23b), and (23c) become

$$\frac{\partial f_0}{\partial \bar{t}}=-i\theta f_0-(f_0-Y)-2Cp_0+ia\frac{\partial^2 f_0}{\partial \bar{x}^2} , \quad (34a)$$

$$\frac{\partial p_0}{\partial \bar{t}}=\bar{\gamma}_\perp[f_0 d_0-(1+i\Delta)p_0] , \quad (34b)$$

$$\frac{\partial d_0}{\partial \bar{t}}=-\bar{\gamma}_\parallel[\tfrac{1}{2}(f_0 p_0^*+f_0^* p_0)+d_0-1] , \quad (34c)$$

where

$$a=\frac{1}{4\pi T\mathcal{F}}, \quad \mathcal{F}=\frac{b^2}{\lambda L} , \quad (35)$$

with $\mathcal{F}$ being the Fresnel number and

$$\overline{\gamma}_\perp=\gamma_\perp/k, \quad \overline{\gamma}_\parallel=\gamma_\parallel/k \ . \tag{36}$$

In the last term of Eq. (30) we replaced k_0 by k_c, as it is appropriate in the limit $\delta_0\to 0$ [see Eqs. (16) and (10)]. Similarly, using Eq. (11'), we find that Eqs. (31), (25b), and (25c) give

$$\frac{\partial f_0}{\partial \overline{t}}=-i\theta f_0-(f_0-Y) -2C\frac{1}{2\pi}\int_{-\pi}^{\pi}d\eta\cos(\eta)p_0(\overline{x},\eta,\overline{t})+ia\frac{\partial^2 f_0}{\partial \overline{x}} \ , \tag{36a}$$

$$\frac{\partial p_0}{\partial \overline{t}}=\gamma_\perp[2f_0 d_0(\overline{x},\eta,\overline{t})\cos\eta-(1+i\Delta)p_0] \ , \tag{36b}$$

$$\frac{\partial d_0}{\partial \overline{t}}=-\overline{\gamma}_\parallel[(f_0 p_0^*+f_0^* p_0)\cos\eta+d_0-1] \ , \tag{36c}$$

where the parameter a is now defined as

$$a=\frac{1}{2\pi\mathcal{F}T} \ . \tag{35'}$$

Because our model requires that $T\ll 1$ [see Eq. (16)], and we want that a remain arbitrary, we complete the definition (16) of the mean-field limit by requiring also that

$$\mathcal{F}\gg 1 \quad (\mathcal{F}T \text{ arbitrary}) \ , \tag{37}$$

which, together with Eqs. (16) and (17), defines the *generalized mean-field limit.*

VII. LINEAR STABILITY ANALYSIS

In the remaining part of this paper we focus on Eqs. (34) for a ring cavity. The quantities f_0^*, p_0^* obey the complex conjugate of Eqs. (34a) and (34b), respectively. Let us now linearize Eqs. (34) around a homogeneous stationary solution. We set

$$\begin{aligned} f_0(\overline{x},\overline{t})&=f_{0,s}+\delta f(\overline{x},\overline{t}) \ , \\ f_0^*(\overline{x},\overline{t})&=f_{0,s}^*+\delta f^*(\overline{x},\overline{t}) \ , \end{aligned} \tag{38}$$

where $f_{0,s}$ is a homogeneous stationary solution which satisfies Eq. (27), and similarly for p_0, p_0^*, and d_0. The linearized set of equations for the quantities δf, δf^*, δp, δp^*, and δd reads

$$\frac{\partial \delta f}{\partial \overline{t}}=-(1+i\theta)\delta f-2C\delta p+ia\frac{\partial^2 \delta f}{\partial \overline{x}^2} \ , \tag{39a}$$

$$\frac{\partial \delta f^*}{\partial \overline{t}}=-(1-i\theta)\delta f^*-2C\delta p^*-ia\frac{\partial^2 \delta f^*}{\partial \overline{x}^2} \ , \tag{39b}$$

$$\frac{\partial \delta p}{\partial \overline{t}}=\overline{\gamma}_\perp[f_{0,s}\delta d+d_{0,s}\delta f-(1+i\Delta)\delta p] \ , \tag{39c}$$

$$\frac{\partial \delta p^*}{\partial \overline{t}}=\overline{\gamma}_\perp[f_{0,s}^*\delta d+d_{0,s}\delta f^*-(1-i\Delta)\delta p^*] \ , \tag{39d}$$

$$\frac{\partial \delta d}{\partial \overline{t}}=-\overline{\gamma}_\parallel[\tfrac{1}{2}(f_{0,s}\delta p^*+p_{0,s}^*\delta f+f_{0,s}^*\delta p +p_{0,s}\delta f^*)+\delta d] \ . \tag{39e}$$

Next, we introduce the following ansatz:

$$\begin{pmatrix} \delta f(\overline{x},\overline{t}) \\ \delta f^*(\overline{x},\overline{t}) \\ \delta p(\overline{x},\overline{t}) \\ \delta p^*(\overline{x},\overline{t}) \\ \delta d(\overline{x},\overline{t}) \end{pmatrix} =\exp(\lambda\overline{t})\cos(\pi n\overline{x}) \begin{pmatrix} \delta f_n \\ \delta f_n^* \\ \delta p_n \\ \delta p_n^* \\ \delta d_n \end{pmatrix} , \tag{40}$$

which assumes that the perturbation δf has the configuration of the transverse mode labeled by n. On inserting Eq. (40) into Eqs. (39) and defining

$$a(n)=a\pi^2 n^2 \ , \tag{41}$$

we obtain the following set of algebraic homogeneous equations:

$$\lambda\delta f_n=-\{1+i[\theta+a(n)]\}\delta f_n-2C\delta p_n \ , \tag{42a}$$

$$\lambda\delta f_n^*=-\{1-i[\theta+a(n)]\}\delta f_n^*-2C\delta p_n^* \ , \tag{42b}$$

$$\lambda\delta p_n=\overline{\gamma}_\perp[f_{0,s}\delta d_n+d_{0,s}\delta f_n-(1+i\Delta)\delta p_n] \ , \tag{42c}$$

$$\lambda\delta p_n^*=\overline{\gamma}_\perp[f_{0,s}^*\delta d_n+d_{0,s}\delta f_n^*-(1-i\Delta)\delta p_n^*] \ , \tag{42d}$$

$$\lambda\delta d_n=-\overline{\gamma}_\parallel[\tfrac{1}{2}(f_{0,s}\delta p_n^*+p_{0,s}^*\delta f_n +f_{0,s}^*\delta p_n+p_{0,s}\delta f_n^*)+\delta d_n] \ , \tag{42e}$$

which, using Eqs. (26), leads to a fifth-order characteristic equation for the eigenvalues:

$$\lambda^5+a_4^{(n)}\lambda^4+a_3^{(n)}\lambda^3+a_2^{(n)}\lambda^2+a_1^{(n)}\lambda+a_0^{(n)}=0 \ , \tag{43}$$

where the explicit expressions of the coefficients $a_i^{(n)}$ $(i=1,2,3,4)$ are given in Appendix A.

The homogeneous stationary solution is stable, provided that all solutions of Eq. (43) have a negative real part, for all values of n. The conditions for the rise of an instability are determined by the Routh-Hurwitz criterion.[20] Here we are mainly interested in the instability which leads to the rise of a spatial pattern. The boundary for this instability is identified by the vanishing of an eigenvalue λ, hence it is characterized by the condition $a_0^{(n)}=0$ with $n\neq 0$. The domain in parameter space where the transversally homogeneous stationary solution in unstable against the growth of a spatial pattern is given by the Routh-Hurwitz inequality

$$a_0^{(n)}\le 0 \quad \text{for } n\neq 0 \ , \tag{44}$$

which, using Eq. (A7) in the Appendix, reads explicitly as

$$\left[1+\frac{2C}{1+\Delta^2+I}\right]\left[1+\frac{2C(1+\Delta^2-I)}{(1+\Delta^2+I)^2}\right]+\left[\theta+a(n)-\frac{2C\Delta}{1+\Delta^2+I}\right]\times\left[\theta+a(n)-\frac{2C\Delta(1+\Delta^2-I)}{(1+\Delta^2+I)^2}\right]\leq 0 \quad (45)$$

and has the solution

$$a^{(-)}\leq a(n)\leq a^{(+)}, \quad (46a)$$

$$a_n^{(\pm)}=-\theta+(1+\Delta^2+I)^{-2}\times(2C\Delta(1+\Delta^2)\pm\{-[I^2+(1+\Delta^2)(1+\Delta^2+2C+2I)]^2+4C^2(1+\Delta^2)I^2\}^{1/2}) . \quad (46b)$$

The meaning of Eq. (46) is that, for a given steady-state intensity I such that the numbers $a^{(\pm)}$ are real, all the transverse modes [given by Eq. (41) with $n>0$] which satisfy condition (46) grow from an initial small value, and thus make the stationary solution unstable. In other words, the transversally homogeneous stationary solution, which corresponds to the value I of the transmitted intensity, is unstable provided that at least one transverse mode $a(n)=a\pi^2n^2$ (with $n>0$) lies in the interval specified by Eq. (46).

If we plot $a^{(+)}$ and $a^{(-)}$ as a function of I, we obtain a bounded region in the plane $(a(n),I)$ that we will call the "instability domain." Here we treat $a(n)$ as a continuous variable. Actually, because by definition $a(n)>0$ $(n>0)$, only the part of this region contained in the upper half plane in meaningful. However, for the considerations given in Sec. VIII, it is useful to consider the whole region.

The instability domain is bounded by the two values I_+ and I_- $(I_-<I_+)$ for which the square root in Eq. (46b) vanishes, so that $a^{(+)}$ and $a^{(-)}$ coincide. Thus I_+ and I_- are the two solutions of the equation

$$I^2+(1+\Delta^2)(1+\Delta^2+2C+2I)=2C(1+\Delta^2)^{1/2}I , \quad (47)$$

which gives

$$I_\pm=[C(1+\Delta^2)^{1/2}-1-\Delta^2]\pm(C(1+\Delta^2)\{C-2[1+(1+\Delta^2)^{1/2}]\})^{1/2} . \quad (48)$$

The instability domain vanishes for $C=2[1+(1+\Delta^2)^{1/2}]$, i.e., when the boundaries I_+ and I_- coincide. Hence the spatial instability can exist only for

$$C>2[1+(1+\Delta^2)^{1/2}] ; \quad (49)$$

the region of the plane (C,Δ^2) identified by condition (49) is shown in Fig. 4. Note that condition (49) does not depend on θ. Clearly, the threshold value of C for the instability is 4, as we see from Fig. 4 for $\Delta=0$. In this sense, the threshold in C for the spatial instability coincides with the bistability threshold (see Sec. IV). Figure 5 shows the boundaries I_+ and I_- as a function of C for a few values of Δ.

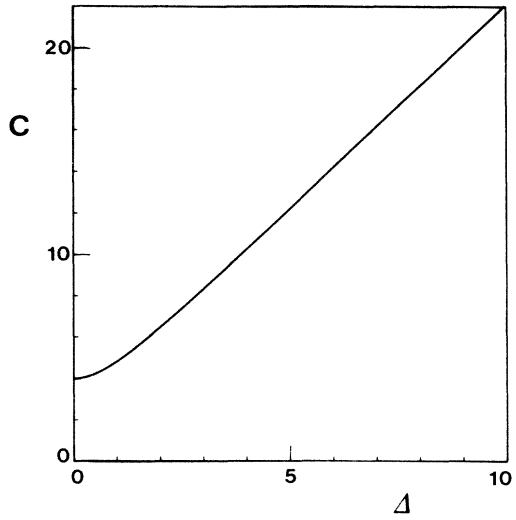

FIG. 4. Plot of the function $C=2[1+(1+\Delta^2)^{1/2}]$. For each value of the atomic detuning Δ, the spatial instability can arise only when the bistability parameter C is larger than the value indicated by this curve.

VIII. GENERAL PROPERTIES OF THE INSTABILITY DOMAIN

The connection between spatial instabilities and bistability, discovered in Sec. VII, is explained by the following two considerations. (1) For $n=0$ [i.e., $a(n)=0$] the instability conditions can be reformulated in the following way:

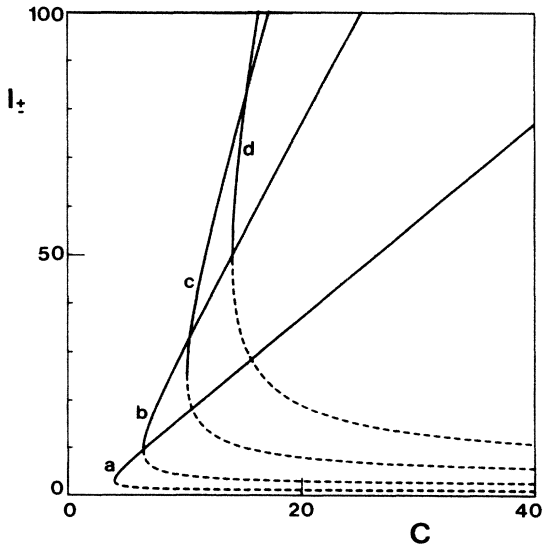

FIG. 5. Boundaries I_- (dashed lines) and I_+ (solid lines) of the instability domain [see Eq. (48)] graphed as a function of the bistability parameter C for several values of the atomic detuning: a, $\Delta=0$; b, $\Delta=\pm2$; c, $\Delta=\pm4$; d, $\Delta=\pm6$.

$$\frac{dY^2}{dI} < 0 , \tag{50}$$

as one can verify immediately using Eqs. (44), (45), and (28). (2) The instability condition (45) depends on θ and $a(n)$ only via the combination $\theta + a(n)$.

From consideration (1) we have immediately that the intersection of the instability domain with the I axis corresponds to the negative-slope segment of the steady-state curve of I as a function of Y^2 [see Eq. (28)]. In particular, the two boundary points of the intersections coincide with the turning points $I_\downarrow$ and $I_\uparrow$ of the steady-state curve (Fig. 6).

Second, by combining points (1) and (2) we find that the instability domain corresponds to the following simple construction procedure: For any given value of $a(n)$, treated as a continuous variable, one considers the interval of the variable I which corresponds to the negative-slope portion of the steady-state curve, given by Eq. (28) with θ replaced by $\theta + a(n)$. Thus one obtains a horizontal segment in the plane $(a(n), I)$. The set of all these segments, obtained for all values of $a(n)$ treated as a continuous variable, gives the instability domain.

This consideration allows us to understand immediately why there is no spatial instability for $C < 4$. In fact, for $C < 4$ there is no negative-slope part in the steady-state curve for any value of the detuning parameter. Similarly one understands why the instability domain is bounded: the negative-slope interval is bounded for any value of $\theta + a(n)$ and vanishes when $|a(n)|$ becomes large enough.

We note that the instability domain is independent of the relaxation rates k, $\gamma_\perp$, and $\gamma_\parallel$, and depends only on the parameters C, Δ, and θ. We note that the existence of a nonvoid instability domain is not sufficient to guarantee the possibility of a spatial instability. First of all, it is necessary that a part of the instability domain is in the upper half plane $a(n) > 0$ so that, by adjusting the diffraction parameter a, one or more transverse modes, given by Eq. (41) with $n > 0$, can be accommodated in the instability domain. As we see from Eq. (35), the parameter a can be varied, for example, by changing the dimensions L and b of the cavity or the transmissivity T of the longitudinal mirrors. Second, the spatial instability can be observed only if it arises in a positive-slope portion of the steady-state curve for the given values of C, Δ, and θ. Hence it is necessary that the width $(I_+ - I_-)$ of the instability domain is larger than the width $(I_\uparrow - I_\downarrow)$ of the negative-slope interval (by construction one has that $I_+ - I_- \geq I_\uparrow - I_\downarrow$, but we need $I_+ - I_- > I_\uparrow - I_\downarrow$). In such a way, one has a spatial instability in the positive-slope domain $I_- < I < I_\downarrow$ or $I_\uparrow < I < I_+$ (Fig. 7).

In the resonant case $\Delta = \theta = 0$, there is no positive-slope spatial instability because $I_- = I_\downarrow$ and $I_+ = I_\uparrow$ (Fig. 8). In the other cases, as it is proven in Appendix B one has the following picture, assuming that C fulfills condition (49). For $\theta \leq 0$ and $\Delta \geq 0$ there is always a positive-slope spatial instability in the intervals $I_- < I < I_\downarrow$ and $I_\uparrow < I < I_+$ (Figs. 6 and 7). For $\theta < 0$ and $\Delta < 0$ there is a positive-slope spatial instability in the portions of the intervals $I_- < I < I_\downarrow$ and $I_\uparrow < I < I_+$ (if any) which satisfy the condition

$$I > -1 - \Delta^2 + [2C\Delta\theta^{-1}(1+\Delta^2)]^{1/2} . \tag{51}$$

For $\theta \geq 0$ and $\Delta \leq 0$ there is never a positive-slope spatial instability. For $\theta > 0$ and $\Delta > 0$ there is a positive-slope spatial instability in the portions of the intervals $I_- < I < I_\downarrow$ and $I_\uparrow < I < I_+$ (if any) which satisfy the condition

$$I < -1 - \Delta^2 + [2C\Delta\theta^{-1}(1+\Delta^2)]^{1/2} . \tag{52}$$

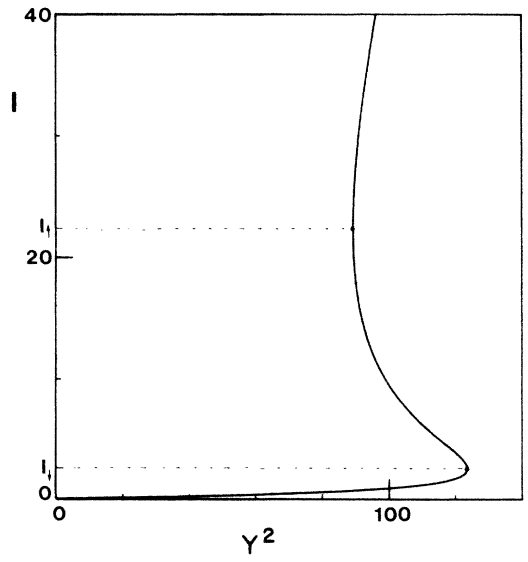

FIG. 6. Steady-state curve of transmitted intensity I as a function of input intensity Y^2 [see Eq. (28)] for $C = 10$, $\Delta = 1$, $\theta = 0$.

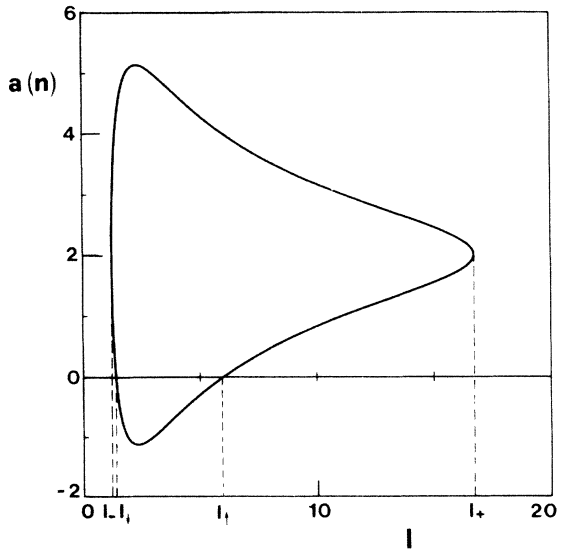

FIG. 7. Domain of the spatial instability in the plane of the variables $a(n)$ and I for $C = 10$, $\Delta = 0$, $\theta = -2$. The positive-slope instability intervals for the variable I are $I_- < I < I_\downarrow$ and $I_\uparrow < I < I_+$.

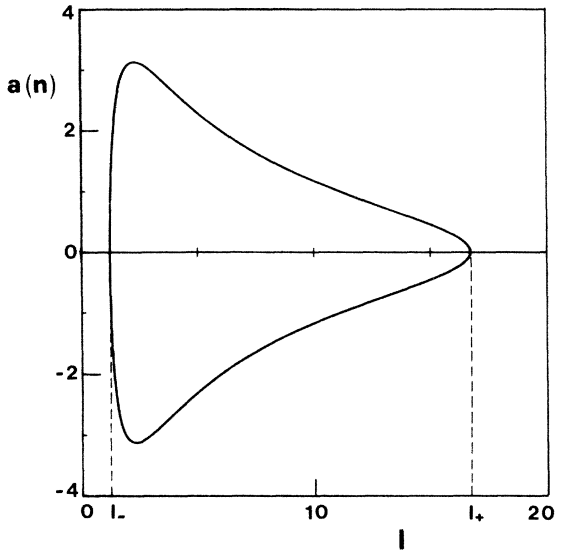

FIG. 8. Same as Fig. 7 for $C=10$, $\Delta=\theta=0$.

In all these cases, when the steady-state curve is not S shaped the phrase "intervals $I_- < I < I_\downarrow$ and $I_\uparrow < I < I_+$" must be replaced by the phrase "interval $I_- < I < I_+$." Note that the expressions (51) and (52) are positive for $C > \theta(1+\Delta^2)(2\Delta)^{-1}$.

In the resonant case $\Delta=\theta=0$, the instability domain is symmetrical with respect to the I axis (Fig. 8); in the other cases it is asymmetrical, and the transformation $\Delta \to -\Delta$, $\theta \to -\theta$ corresponds to a π rotation around the I axis [see Fig. 9 and Eq. (46)].

The property (2) has also another important consequence, namely a change of the parameter θ corresponds simply to a translation of the instability domain parallel to the vertical axis. Precisely a decrease (increase) of θ corresponds to a translation in the upward (downward) direction; compare, for instance, Figs. 7 and 8. Therefore, when condition (49) is satisfied, a positive-slope spatial instability is guaranteed provided that θ is made negative enough. Simultaneously, the steady-state curve loses its S-shaped character (Fig. 10). Conversely, when θ is positive and is increased enough, the possibility of spatial instability vanishes because the instability domain lies entirely in the lower half plane $a(n) < 0$.

This simple translation property of the instability domain under a variation of θ implies that, for given values of C and Δ, it is enough to plot the instability domain for one value of θ, for example, $\theta=0$. We finish this section with three remarks.

(i) The spatial instability is possible also in absence of bistability, i.e., when the steady-state curve is not S shaped, see Fig. 10.

(ii) The spatial instability can occur both in the lower and upper branch of the steady-state curve (see Fig. 7).

(iii) When condition (49) is fulfilled, for $\Delta > 0$ (self-defocusing case), the spatial instability is also there for $\theta=0$, whereas for $\Delta < 0$ (self-focusing case) it is possible only when θ is negative enough. In this sense, the instability is "easier" in the self-defocusing case.

IX. TEMPORAL AND SPATIO-TEMPORAL STRUCTURES

The other Routh-Hurwitz conditions,[20] different from (44), identify instabilities which may lead to the rise of temporal structures for $a(n)=0$, or to the rise of spatio-temporal structures for $a(n) > 0$. In fact, all the other instability boundaries different from that defined by condition $a_0^{(n)}=0$ correspond to the vanishing of the real part of a pair of complex-conjugate eigenvalues. The instabili-

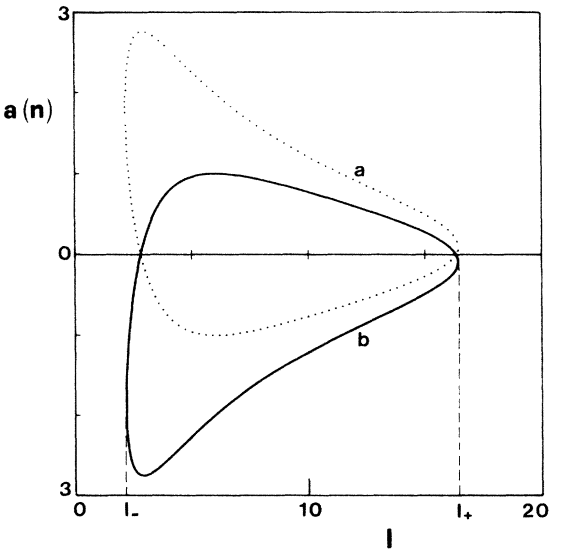

FIG. 9. Same as Fig. 7 for *a*, $C=8$, $\Delta=-1$, $\theta=0$; *b*, $C=8$, $\Delta=1$, $\theta=0$.

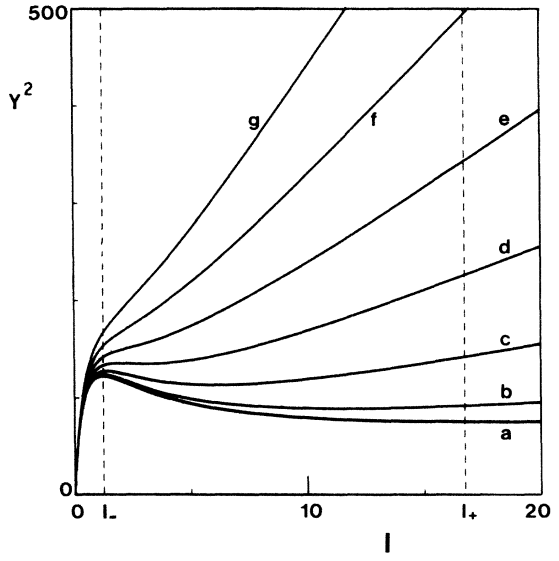

FIG. 10. Steady-state curves of incident intensity Y^2 as a function of transmitted intensity I [see Eq. (28)] for $C=10$, $\Delta=0$, and *a*, $\theta=0$; *b*, $\theta=-1$; *c*, $\theta=-2$; *d*, $\theta=-3$; *e*, $\theta=-4$; *f*, $\theta=-5$; *g*, $\theta=-6$. The positive-slope portion of the curves for $I_- < I < I_+$ is unstable against the onset of a spatial pattern.

ty problem for $a(n)=0$, i.e., neglecting diffraction, has been extensively analyzed in Ref. 21.

Provided the cavity detuning θ is sufficiently removed from zero, one finds extended domains in parameter space which lead to temporal structures. This time, the onset of the instability depends not only on C,Δ, and θ but also on the parameters $k/\gamma_\perp$ and $k/\gamma_\parallel$.

On the basis of these results, we can now prove the existence of instabilities which lead to spatio-temporal structures. In fact, this is an immediate consequence of the circumstance that the eigenvalue equation (43) depends on θ and $a(n)$ only via the combination $\theta+a(n)$. If, for example, one of the Routh-Hurwitz instability conditions different from (44) is satisfied for $\theta=\bar{\theta}>0$ and $a(n)=0$, the same condition is satisfied, e.g., for $\theta=0$ and $a(n)=\bar{\theta}$, thereby producing an instability in a transverse mode, which may lead to the formation of a spatio-temporal structure.

These types of instabilities can be studied in the same way as we did for the purely spatial instability in Sec. VIII. In particular, one can associate them with an instability domain in the plane of the variables $a(n)$ and I, using a construction procedure completely analogous to that described in Sec. VIII, and a variation of θ corresponds to a translation parallel to the axis $a(n)$. The analysis of these types of instabilities is left, however, to future work.

X. ADIABATIC ELIMINATION OF THE ATOMIC VARIABLES

The study of the structures which emerge from the spatial instability displayed by Eqs. (34) becomes easier in the limit

$$\bar{\gamma}_\perp,\bar{\gamma}_\parallel \gg 1 , \tag{53}$$

in which the atomic variables can be eliminated by setting $dp_0/dt=d\,d_0/dt=0$ in Eqs. (34b) and (34c). Thus one obtains the relations

$$p_0=\frac{(1-i\Delta)f_0}{1+\Delta^2+|f_0|^2},\quad d_0=\frac{1+\Delta^2}{1+\Delta^2+|f_0|^2} , \tag{54}$$

and the self-contained equation for f_0,

$$\frac{\partial f_0}{\partial \bar{t}}=Y-f_0\left[\left(1+\frac{2C}{1+\Delta^2+|f_0|^2}\right)+i\left(\theta-\frac{2C\Delta}{1+\Delta^2+|f_0|^2}\right)\right]+ia\frac{\partial^2 f_0}{\partial \bar{x}^2} . \tag{55}$$

We note that the set of stationary solutions (transversally uniform and nonuniform) of Eq. (34) coincides exactly with the set of stationary solutions of Eq. (55); however, their stability depends on the parameters $\bar{\gamma}_\perp$ and $\bar{\gamma}_\parallel$. The linear-stability analysis of the transversally homogeneous stationary solution, based on Eq. (55) valid in the limit (53), can be performed in the usual way. It leads to the quadratic eigenvalue equation

$$\lambda^2+2\lambda+a_0^{(n)}(\bar{\gamma}_\perp^2\bar{\gamma}_\parallel D)^{-1}=0 , \tag{56}$$

where the expression $a_0^{(n)}$ is given by Eq. (A7) in Appendix A. Clearly, Eq. (56) can never display two roots with a positive real part, hence the possibility of temporal or spatio-temporal structures is excluded in the model (55). On the other hand, Eq. (55) exhibits the same spatial structures of the original model (34), and the related instability condition is still given by Eq. (44). Hence, all the consideration given in Sec. VIII hold unchanged for Eq. (55), which will be analyzed in detail in part II of this article.

XI. PHYSICAL INTERPRETATION OF THE INSTABILITY

In this section we want to illustrate the physical origin of our instability. For the sake of definiteness, let us refer to the cavity configuration of Fig. 3 (Fabry-Perot–type). The frequency of the cavity mode characterized by the wave vector components k_x, k_c is usually given as

$$\omega=c(k_x^2+k_c^2)^{1/2}$$

In our case we assume that $k_x \ll k_z$. Hence we obtain

$$\omega=ck_c+\Delta\omega,\quad \Delta\omega=\frac{c}{2k_c}k_x^2 , \tag{57}$$

where $\Delta\omega$ is the transverse contribution to the mode frequency. In Eq. (31), this contribution arises from the term

$$i\frac{c}{2k_0}\frac{\partial^2 f_0}{\partial x^2} ;$$

on substituting $f_0\propto\cos(k_x x)$ we recover the expression (57) of $\Delta\omega$, with k_c replaced by k_0; the replacement of k_0 by k_c is explained in the sentence after Eq. (36). These considerations give an intuitive explanation of the coefficient $c/2k_0$ in Eq. (31). If we now take into account that $k_x=\pi n/b$, $k_c=2\pi/\lambda$, we obtain, from Eq. (57),

$$\Delta\omega_n=\frac{c\pi\lambda}{4b^2}n^2 . \tag{58}$$

Let us now consider the ratio $\Delta\omega/k$, where the cavity linewidth k is defined by Eq. (11′). Using Eq. (35′) we get

$$\frac{\Delta\omega_n}{k}=a\pi^2n^2=a(n) . \tag{59}$$

In Sec. V we introduced the generalized mean-field limit $T\ll 1$, $\mathcal{F}\gg 1$, with $a\propto(T\mathcal{F})^{-1}$ arbitrary. This allows to have $a(n)$ of order unity, which implies that $\Delta\omega_n$ and k have the same order of magnitude.

If we consider only the longitudinal modes of cavity ($n=0$), for $T\ll 1$ the modes are well separated, and therefore the input field selects the nearest mode (resonant mode). Hence only one mode contributes to the stationary state. On the other hand, as we just showed, when $a(n)$ is of the order of unity, there are transverse modes whose frequency distance $\Delta\omega_n$ from the resonant

homogeneous mode is on the order of the modal width k. Therefore these modes compete with the resonant mode, and via the instability give rise to a new stationary state which presents *spatial coexistence of modes.* This is very different from the *temporal coexistence of longitudinal modes,* which arises in multimode instabilities, that via Hopf bifurcation lead to oscillatory or self-pulsing behavior.[1] In this paper we pointed out a new kind of multimode instability, which leads to time-independent spatial pattern formation. In this connection, we observe that the analysis of this paper is in a sense complementary to that of Ref. 22. Actually, the configuration considered in Ref. 22 is different because the medium is active and not passive, there is no input field, and the cavity is a standard ring cavity with spherical mirrors. However, the two works have in common the fact of studying the competition between a longitudinal mode and the corresponding set of transverse modes. Contrary to the situation considered in this paper, in Ref. 22 the parameters are selected in such a way that the transverse modes are well separated from the longitudinal mode. As a consequence, the instabilities which arise there produce the onset of spontaneous oscillations, with temporal coexistence of transverse and longitudinal modes, instead of producing the formation of a stationary spatial pattern.

Our analysis is presumably related to the known results on self-focusing and filamentation of light beams in nonlinear media.[23,24] This was made easier by the pioneering works on spatial solitons[13] and modulational instabilities[19] by Moloney and collaborators. The analysis of the relations between these results and our remains as a main focus of investigation.

The spatial solutions are stationary spatial patterns, but the usual description of their origin is not related to spatial dissipative structures. In fact, they arise from the up switching of the central portion of a Gaussian beam, which creates large gradients in the transverse profile. On the other hand, our instability is not at all related to the switching points, and does not even require a bistable steady-state curve. One cannot exclude that by performing a linear-stability analysis of the model of Ref. 13 in the upper branch, one may discover an instability which gives rise to a spatial dissipative structure, and show that this structure is precisely the spatial soliton. All of this entirely remains, however, to be studied.

The treatment of modulational instabilities in Ref. 19 is general; the instabilities analyzed in that work lead, however, to dynamical oscillations. It is not all unreasonable to hope that under different conditions, the same theory can give rise to stationary spatial structures; again this remains to be proven.

On the other hand, our model exhibits, in an explicit, exact, and analytic way, the onset of a stationary spatial dissipative structure in an optical system. In order to achieve this goal most simply we used the mean-field limit and introduced the lateral mirrors, which produce a discrete set of transverse modes. Our analysis points out the crucial fact that the stationary spatial structure arises when the frequency distance between the transverse modes and the resonant longitudinal mode is on the order of the cavity linewidth.

XII. CONCLUDING REMARKS

Our results predict that a plane-wave input field can be spontaneously converted into a stationary beam which presents a transverse stripe structure. Of course this structure has nothing to do with the usual diffraction fringes from a slit; the width of the stripes is given by b/n, where b is the lateral length of the cavity and n is a small integer, and is therefore much larger than the wavelength.

Our analysis provides an example of Turing instability[25] that arises from a model which is not only simple but also, hopefully, realizable experimentally. This is in contrast with the situation of chemical and biological models, in which it appears exceedingly difficult to reconcile simplicity with a sufficient degree of realism. Hence an experimental observation of the phenomenon predicted in this paper would be of great interest.

As we mentioned in Sec. XI, our plan was to formulate an optical model which exhibits, in the most clearcut and analytical way, the phenomenon of spontaneous spatial pattern formation. Hence we selected a model that admits a transversally homogeneous stationary solution in order to show that under appropriate conditions this state can be destabilized and converted into a stationary spatial structure. A phenomenon of the same kind would be, for example, the formation of stationary modulational patterns on a broad Gaussian envelope; this configuration does not allow, however, for an exact analytical treatment.

For this reason we considered a cavity that can accomodate an input plane wave. This is ensured by the reflecting boundary conditions on the mirrors orthogonal to the axis x because they lead to a cosine structure for the cavity modes with respect to the transverse variable x [see Eqs. (32a) and (32b)]; in particular, the mode with $n=0$ corresponds to a uniform transverse configuration. On the contrary, this is not possible if the modes have, for example, a sine structure in x. We observe in this connection that on the other hand, the cosine configuration with respect to the longitudinal variable z, assumed for the Fabry-Perot modes in Eq. (32b), is completely irrelevant for our treatment. A sine structure with respect to z is equally admissible, and does not change anything in our analysis.

The reflecting boundary conditions for x can be realized, at least approximately, by coating the sides of the sample orthogonal to the axis by a dielectric layer with a refractive index larger than that of the sample itself. We note furthermore that the electric field polarization that we consider was selected because it allows for an exact treatment of the problem. On the other hand, the choice of an electromagnetic field linearly polarized, with the *magnetic* field oriented in the y direction, allows for a simple realization by means of a cavity with conducting walls.[26] In this case, again Maxwell's equations imply that E does not depend on y. The mode configuration for the component E_x is $\cos(k_x x)\sin(k_c z)$. For $k_x \neq 0$ there is also a component $E_z \propto \sin(k_x x)\cos(k_c z)$, but this is extremely small because $|E_z/E_x| = k_x/k_c$ and the condition $k_x/k \ll 1$ is already assumed in the derivation of Eq.

(5a). Neglecting E_z, our previous treatment remains completely unchanged.

In order to obtain a plane-wave configuration for the input beam, it is necessary to magnify it by lenses and use only its central part. This means a loss of intensity. However, the power requirements for the observation of this instability are not severe because the instability threshold is lower than the bistability threshold.

ACKNOWLEDGMENTS

The research was carried out in the framework of the European Economic Community twinning project on dynamics of nonlinear optical systems. We are grateful to Professor G. Leuchs and Professor G. Bava for illuminating discussions.

APPENDIX A

Let us specify the coefficients $a_i^{(n)}$ $(i=1,2,3,4)$ in the eigenvalue equation (43). By setting

$$\theta_n=\theta+a(n)=\theta+a\pi^2n^2 \tag{A1}$$

and

$$\mathcal{D}=1+\Delta^2+I\ , \tag{A2}$$

with I defined by Eq. (28'), we have

$$a_4^{(n)}=2+\bar{\gamma}_\parallel+2\bar{\gamma}_\perp\ , \tag{A3}$$

$$a_3^{(n)}=\bar{\gamma}_\parallel\bar{\gamma}_\perp(2+I)+1+\theta_n^2+2(\bar{\gamma}_\parallel+2\gamma_\perp^2)+\bar{\gamma}_\perp^2(1+\Delta^2)+4C\bar{\gamma}_\perp(1+\Delta^2)/\mathcal{D}\ , \tag{A4}$$

$$a_2^{(n)}=\bar{\gamma}_\perp^2\bar{\gamma}_\parallel\mathcal{D}+2\bar{\gamma}_\perp\bar{\gamma}_\parallel(2+I)+2\bar{\gamma}_\perp^2(1+\Delta^2)+(\bar{\gamma}_\parallel+2\bar{\gamma}_\perp)(1+\theta_n^2)+4C\bar{\gamma}_\perp(\bar{\gamma}_\perp+\bar{\gamma}_\parallel+1)(1+\Delta^2)\mathcal{D}^{-1}-2C\bar{\gamma}_\perp\bar{\gamma}_\parallel I\mathcal{D}^{-1}\ , \tag{A5}$$

$$\begin{aligned}a_1^{(n)}=&2\bar{\gamma}_\parallel\bar{\gamma}_\perp^2\mathcal{D}+\bar{\gamma}_\parallel\bar{\gamma}_\perp(1+\theta_n^2)(2+I)+\bar{\gamma}_\perp^2(1+\theta_n^2)(1+\Delta^2)+4C\bar{\gamma}_\perp(\bar{\gamma}_\parallel+\bar{\gamma}_\perp+\bar{\gamma}_\parallel\bar{\gamma}_\perp)(1+\Delta^2)\mathcal{D}^{-1}\\&-4C\bar{\gamma}_\perp^2\theta_n\Delta(1+\Delta^2)\mathcal{D}^{-1}+4C^2\bar{\gamma}_\perp^2(1+\Delta^2)^2\mathcal{D}^{-2}-2C\bar{\gamma}_\perp\bar{\gamma}_\parallel(1+\theta_n\Delta)\mathcal{D}^{-1}\ ,\end{aligned} \tag{A6}$$

$$a_0^{(n)}=\bar{\gamma}_\perp^2\bar{\gamma}_\parallel\mathcal{D}\{(1+2C\mathcal{D}^{-1})[1+2C(1+\Delta^2-I)\mathcal{D}^{-2}]+(\theta_n-2C\Delta\mathcal{D}^{-1})[\theta_n-2C\Delta(1+\Delta^2-I)\mathcal{D}^{-2}]\}\ . \tag{A7}$$

APPENDIX B

The expression of the boundaries $a^{(+)}$ and $a^{(-)}$ of the instability domain, given by Eq. (46), can be rephased as follows:

$$a^{(\pm)}=\frac{2C\Delta(1+\Delta^2)}{(1+\Delta+I)^2}-\theta \pm\left[\left[\frac{2C\Delta(1+\Delta^2)}{(1+\Delta^2+I)^2}-\theta\right]^2-\frac{dY^2}{dI}\right]^{1/2}\ , \tag{B1}$$

where the expression of dY^2/dI is given by the left-hand side of Eq. (45) for $a(n)=0$. Let us now consider the positive-slope parts $(dY^2/dI>0)$ of the interval $I_-<I<I_+$ where the quantities $a^{(\pm)}$ are defined. A spatial, positive-slope instability is possible only if $a^{(+)}$ and $a^{(-)}$ are positive. This condition holds if

$$\frac{2C\Delta(1+\Delta^2)}{(1+\Delta^2+I)^2}>\theta\ . \tag{B2}$$

For $\theta=\Delta=0$ the interval $I_-<I<I_+$ does not contain positive-slope intervals. In the other cases, we obtain the following picture. For $\theta\le 0$ and $\Delta\ge 0$, condition (B2) is always satisfied, whereas for $\theta\ge 0$ and $\Delta\le 0$ it is never fulfilled. Condition (B2) leads to Eq. (51) for $\theta<0$ and $\Delta<0$, and leads to Eq. (52) for $\theta>0$ and $\Delta>0$.

[1]See the feature issue on Instabilities in Active Optical Media, J. Opt. Soc. Am. B **2** (1985).

[2]*Optical Instabilities*, edited by R. W. Boyd, M. G. Raymer, and L. M. Narducci (Cambridge University Press, Cambridge, England, 1986).

[3]L. A. Lugiato, in *Progress in Optics*, edited by E. Wolf (North-Holland, Amsterdam, 1984), Vol. XXI, p. 69.

[4]H. J. Carmichael, in *Laser Physics*, Vol. 182 of *Lecture Notes in Physics*, edited by J. D. Harvey and D. F. Walls (Springer-Verlag, Berlin, 1983), p. 64.

[5]P. Mandel, in *Frontiers in Quantum Optics*, edited by R. Pike and S. Sarkar (Hilger, Bristol, 1986), p. 261.

[6]R. G. Harrison and D. J. Biswas, Prog. Quantum Electron. **10**, 147 (1985).

[7]N. B. Abraham, P. Mandel, and L. M. Narducci, in *Progress in Optics*, edited by E. Wolf (North-Holland, Amsterdam, in press).

[8]E. Arimondo, in *Synergetics and Dynamic Instabilities*, edited by G. Caglioti, H. Haken, and L. A. Lugiato (North-Holland, Amsterdam, in press).

[9]H. Haken, *Synergetics—An Introduction* (Springer-Verlag, Berlin, 1977).

[10]G. Nicolis and I. Prigogine, *Self-Organization in Nonequilibrium Systems* (Wiley, New York, 1977).

[11]J. D. Murray, J. Theor. Biol. **88**, 161 (1981).

[12]L. A. Lugiato and R. Lefever, Phys. Rev. Lett. **58**, 2209 (1987).

[13]J. V. Moloney and H. M. Gibbs, Phys. Rev. Lett. **48**, 1607 (1982).

[14]S. W. Koch, H. E. Schmidt, and H. Haug, Appl. Phys. Lett. **45**, 932 (1984).

[15]L. M. Narducci, J. R. Tredicce, L. A. Lugiato, N. B. Abraham, and D. K. Bandy, Phys. Rev. A **32**, 1588 (1985).

[16]L. A. Lugiato and L. M. Narducci (unpublished).

[17]P. D. Drummond, IEEE J. Quantum Electron. **QE-17**, 301 (1981).

[18]H. J. Carmichael and J. A. Hermann, Z. Phys. B **38**, 365 (1980).
[19]D. W. McLaughlin, J. V. Moloney, and A. C. Newell, Phys. Rev. Lett. **54**, 681 (1985).
[20]M. Marden, *The Geometry of the Zeroes of a Polynomial in a Complex Variable, Mathematical Surveys* (American Mathematical Society, New York, 1949), Vol. III.
[21]L. A. Lugiato, R. J. Horowicz, G. Strini, and L. M. Narducci, Phys. Rev. A **30**, 1366 (1984).
[22]L. A. Lugiato, F. Prati, L. M. Narducci, P. Ru, J. Tredicce, and D. K. Bandy (unpublished).
[23]V. I. Bespalov and V. I. Talanov, Pis'ma Zh. Eksp. Teor. Fiz. **14**, 564 (1971) [JETP Lett. **14**, 390 (1971)]; Zh. Eksp. Teor. Fiz. **60**, 136 (1971) [Sov. Phys.—JETP **33**, 77 (1971)].
[24]K. Konno and H. Suzuki, Phys. Scr. **20**, 382 (1979).
[25]A. M. Turing, Philos. Trans. R. Soc. London, Ser. B **237**, 37 (1952).
[26]N. Marcuvitz, *Waveguide Handbook* (McGraw-Hill, New York, 1951), p. 64.

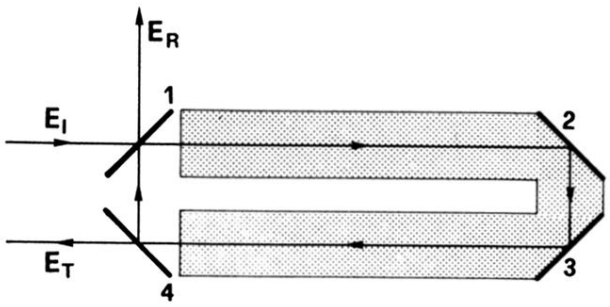

FIG. 1. Ring cavity filled with a passive medium. Mirrors 1 and 4 have transmissivity coefficient $T \ll 1$, mirrors 2 and 3 have 100% reflectivity. E_I, E_T, and E_R are the incident, transmitted, and reflected fields, respectively.